Specular Effects of Shuttle Orbiter Radiators on a Typical Payload

L.D. Turner,* W.R. Humphries,† and J.W. Littles‡
NASA Marshall Space Flight Center, Alabama

Analyses performed to determine the Space Shuttle's payload bay thermal environment generally consider all external surfaces of the Orbiter and its payload to reflect energy diffusely. However, the Orbiter's active thermal control system (ATCS) radiators utilize highly specular silverized Teflon on their outer surfaces. This study considers solar energy specularly reflected from these radiators on a typical deployed payload which extends outside the payload bay envelope. Parameters investigated include the degree of specularity of the radiators and the solar inclination angle with respect to the radiators. Comparisons are made between payload environmental heat flux levels assuming both diffuse and specular radiators.

Introduction

IN a number of past studies, Space Shuttle Orbiter payload bay thermal environment predictions have considered all Orbiter surfaces to reflect energy diffusely. However, for those payloads in the region influenced by the Orbiter's radiators, this assumption may produce erroneous results. In contrast to being diffuse, the radiators currently are covered with highly specular silverized Teflon material. Also, the upward facing surfaces of the deployed radiators have a concave contour. This shape produces a local concentration of reflected energy on those bodies lying in the region of influence. Consequently, this study examines the combined effect of the Orbiter radiator specularity and geometry on a typical payload located in the affected region.

Diffuse and Specular Energy Reflection

When analyzing reflected energy from a surface, the surface may either be considered 1) diffuse, 2) specular, or 3) a combination of diffuse and specular. The term diffuse refers to a characteristic in which the intensity of energy emitted and reflected from the surface is uniform in all angular directions. In contrast, when the surface is specular, reflected energy rays from that surface have zero radiation intensity in all directions except at a single angle from the normal vector of the reflecting surface. This angle is identical to that formed between the incoming rays and the surface normal. The reflected rays are confined to the plane defined by the surface normal and incoming rays. In reality, most surfaces reflect energy both diffusely and specularly, with the degree of specularity being dependent on such factors as material type, surface finish, incident energy wavelength, and direction of incidence.

The energy spectrum may be divided into infrared (i.e., long wavelength) and solar (i.e., short wavelength) energy bands. Assuming no transparent surfaces, the basic radiation relationships are

$$\alpha_{ir} + \rho_{ir}^{diff} + \rho_{ir}^{spec} = 1 \qquad \alpha_S + \rho_S^{diff} + \rho_S^{spec} = 1$$

where,

α = surface absorptance
ρ = surface reflectance
ir = infrared energy
S = solar energy
diff = diffuse energy component
spec = specular energy component

Problem Description

Orbiter Radiators

As the major source of on-orbit cooling-loop heat rejection, the Orbiter's active thermal control system (ATCS) uses space radiators. These radiators are situated on the inside of the payload bay doors. The radiators, like the doors, are divided approximately equally down the payload bay length into front and back sections. These sections are identified as the starboard and port forward radiators and the starboard and port aft radiators. Each section is composed of two separate radiator panels. These panels are contoured to the shape of the doors, being "cusplike" in cross section (Fig. 1).

After reaching orbit, the doors are opened fully, exposing the radiator surfaces to space. The ATCS heat rejection capability is augmented further by deploying the forward radiators 35.5 deg away from the doors. This action exposes the underside of the forward radiator panels, which, like the aft and forward upper surfaces, are covered with a second surface mirror material.

Radiator Surface

The external surfaces of the radiators are covered with a second surface mirror material (silverized Teflon). The silver undercoating of this material acts with the Teflon cover surface to form a highly efficient heat-rejection material (i.e., low α_S/ϵ_{ir}). However, the silver undersurface causes the material to exhibit a highly specular characteristic in the presence of solar/albedo irradiation.

Shuttle/Spacelab interface documentation[1] indicates the silverized Teflon to be 96 to 99% ρ^{spec} [where $\% \rho^{spec} = 100 \times \rho^{spec}/(\rho^{spec} + \rho^{diff})$] as applied to the radiators. Although the Orbiter radiators will use an embossed silverized Teflon to reduce their specularity after the fifth flight, for the purposes of this study a 100% ρ^{spec} baseline is assumed.

Radiator Curvature

The contour and location of the deployed forward radiator is a central parameter affecting the distribution of reflected energy on a payload in the Orbiter's payload bay. A set of four polynomial equations which were fit to the actual

Presented as Paper 81-1074 at the AIAA 16th Thermophysics Conference, Palo Alto, Calif., June 23-25, 1981; submitted Dec. 21, 1981; revision received June 7, 1982.

*Environmental Control Engineer, Life Support and Environmental Branch, Engineering Analysis Division, Structures and Propulsion Laboratory.

†Chief, Life Support and Environmental Branch, Engineering Analysis Division, Structures and Propulsion Laboratory.

‡Chief, Engineering Analysis Division, Structures and Propulsion Laboratory.

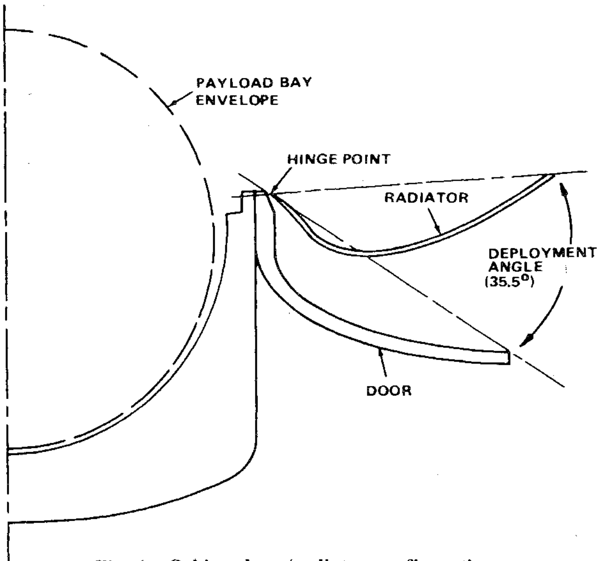

Fig. 1 Orbiter door/radiator configuration.

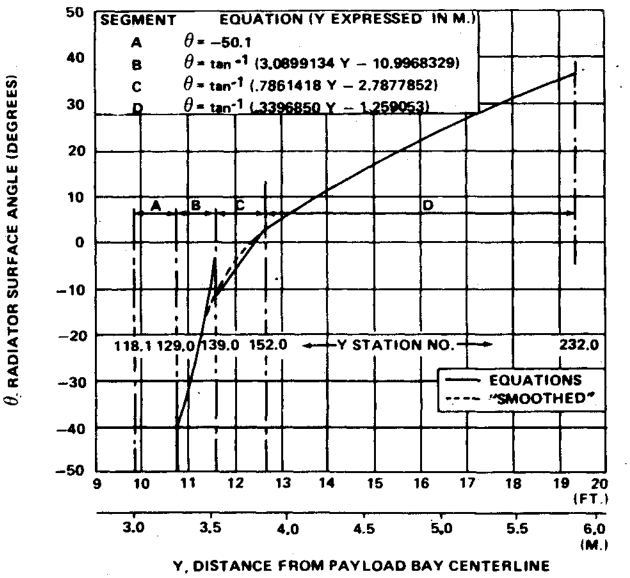

Fig. 2 Orbiter radiator surface angle (aft portion of deployed forward radiator).

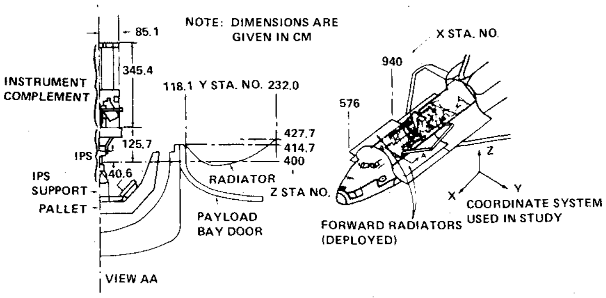

Fig. 3 SL-2 payload and radiator configuration.

radiator contour are used to define the curvature of the forward radiator. Discontinuities at the junctions of the four segments were eliminated by smoothing the plot of the radiator surface angle θ, as shown in Fig. 2.

Payload Configuration

A typical payload configuration was used in this study. The configuration selected was to have its payload in the thermal field of view of the forward radiators (the aft radiators and

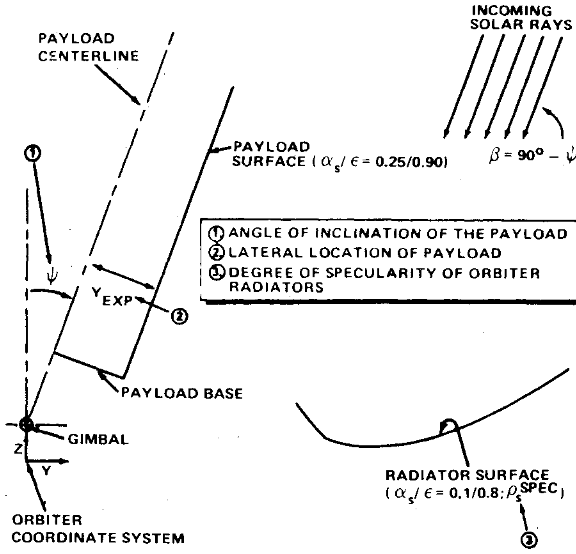

Fig. 4 Parameters investigated.

undeployed forward radiators have little or no thermal effect on payloads because of their limited thermal view of the payload bay region). As shown in Fig. 3, the Spacelab mission 2 (SL-2) forward pallet payload exhibits this characteristic. This payload currently consists of the European Space Agency's instrument pointing system (IPS), the attendant optical sensor package (OSP), the IPS experiment payload complement, and a mounting structure used to interface the IPS structurally with the experiments. The experiment package, taken collectively, is herein referred to as the IPS payload.

The IPS payload is situated in the Orbiter forward payload bay volume. The IPS provides a tiltable platform for experiments, which may either be stowed (i.e., laid horizontally) or deployed to point at the sun or stellar fields. SL-2's primary target is the sun. Because of its elevated position in the bay in the deployed configuration, the IPS payload has an extremely good view of the deployed forward radiators. The IPS payload deployed configuration is shown in Fig. 3, along with the coordinate system utilized in this study. Also shown in this figure is the geometric relationship between the IPS payload and the radiator.

For the purposes of this study, the deployed IPS tilt capability is limited to 40 deg in any direction from the $+z$ axis (i.e., at $\pm$40-deg cone angle from the payload bay normal). Also the IPS line of sight (i.e., instrument pointing direction) is always considered to be directed at the sun.

Parameters Investigated

The radiators can direct solar energy onto the sidewalls of the IPS-mounted instruments. This occurs during the sunlit portion of the orbit in which the vehicle is oriented with its payload bay in the direction of the sun. In general, it is the purpose of this study to determine the differences in the magnitudes of purely diffuse and specularly reflected solar energy levels on a typical Spacelab payload which views the forward radiators.

With the payload pointing in the direction of the sun, the degree to which three parameters affect the amount of reflected solar energy on the payload were investigated in this study. These parameters were 1) the angle of inclination of the payload with respect to the Orbiter $\pm z$ axis (plane of this angle maintained parallel to the yz plane); 2) the lateral position of the payload (i.e., position of the surface on which reflected energy is incident as measured from and maintained parallel to the xz plane); and 3) the degree of specularity ($\%\rho^{\text{spec}}$) of the radiators. These parameters are defined in Fig. 4. The first two of these are mission peculiar since they are influenced by such things as the flight attitude, the payload arrangement (i.e., configuration), and pointing requirements dictated by the science objectives of the mission.

Analytical Approach

Analysis Methods and Assumptions

Complicated radiative environments for Earth-orbiting spacecraft are generally determined using digital computer programs written specifically for that purpose. Two such programs are the Lockheed orbital heat rate package (LOHARP)[2] and the thermal radiation analysis system (TRASYS).[3] These programs allow the user to represent the geometry of the orbiting vehicle by a composition of various geometric shapes (e.g., rectangles, disks, polygons, cones, etc.). Current integration activities for Spacelab missions 1-3 have utilized TRASYS to generate orbital environment data. This program allows the analyst to use several hundred nodes to represent the Orbiter and its payload. The original version of this program (i.e., TRASYS I) is capable of analyzing only totally diffuse surfaces. However, a more recent version, TRASYS II,[4] is capable of analyzing specular/diffuse surfaces. This program was used in the present study. Because the specular portion of the program has had only limited use, additional methods of analyses were also employed. These methods consisted of a simple geometric analysis of incident and reflected rays using a small Fortran program and a statistical method based on random sampling (i.e., Monte Carlo) using a large generalized computer program. In summary, the three methods of analysis used in this study were 1) a generalized thermal radiation program, thermal radiation analysis system (TRASYS II), 2) a specialized specular ray trace program, and 3) a generalized Monte Carlo-based thermal radiation program. In utilizing these programs, the following were assumed.

1) Solar constant = 429.0 Btu/h-ft^2 (1353.1 W/m^2).
2) Radiator solar absorptance = 0.1.
3) Payload solar absorptance = 0.25.
4) The radiator degree of specularity is independent of the angle of the incident energy and local surface irregularities.
5) Only direct solar (i.e., short wavelength) energy is considered to be specularly reflected from the radiators.
6) A planar surface is used to represent the payload.
7) The longitudinal axis of the IPS/payload is maintained parallel to the solar vector (i.e., the payload is always pointed toward the sun).
8) The solar vector is maintained parallel to the yz plane of the Orbiter.
9) With the exception of the Monte Carlo-based thermal radiation program, only one "bounce" per ray of solar energy from the radiator is considered.

The last assumption (i.e., energy is not allowed to reflect from one portion of the radiator onto another portion and then to the payload) could be a severe analytical limitation when dealing with geometries containing pronounced cavities. However, it was considered of no consequence for the rather open radiator/payload geometry in the present study (Fig. 5).

TRASYS II Based Models

Both a "two-dimensional" and three-dimensional TRASYS II based model of the radiator and payload configuration were constructed. The two-dimensional model (actually, a three-dimensional model with extremely narrow dimensions in the x direction) was used only when considering strictly specularly (i.e., $\%\rho^{spec} = 100$) reflected energy from the radiators. The geometry for this two-dimensional model (141 nodes) is shown in Fig. 6. Since TRASYS II allows only planar nodes to be considered as specular reflectors, the radiator was nodalized using 101 narrow, rectangular surfaces. A full three-dimensional model was constructed to permit analyses involving a less than 100% specular radiator. As shown in Figs. 7 and 8, 239 nodes were used to represent the payload and radiator. Since the solar vector was always maintained parallel to the IPS/payload longitudinal axis in this study, only the section of the radiator that would contribute to energy being specularly reflected on the payload was rigorously modeled (i.e., 101 nodes as compared with the 26 nodes used to represent each of the remaining sections). Because the present study was concerned with differences between the total absorbed heating rates on the payload (determined when assuming both specular and diffuse radiators), it was necessary to include the entire forward radiator. Solar energy reflected specularly from the radiator surface can be analyzed two dimensionally because the solar

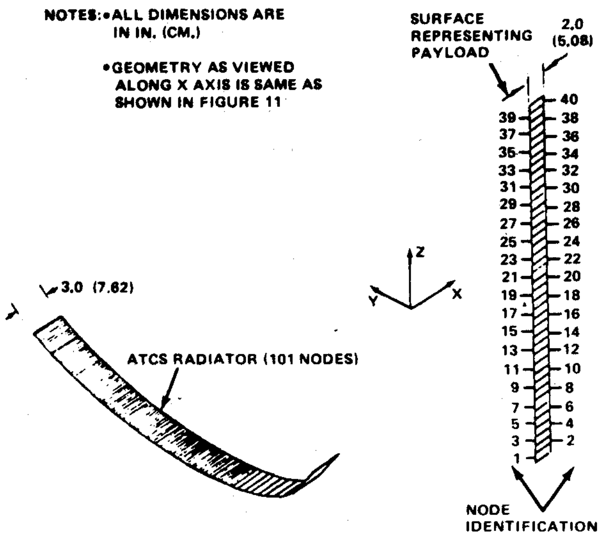

Fig. 6 Two-dimensional TRASYS II based model.

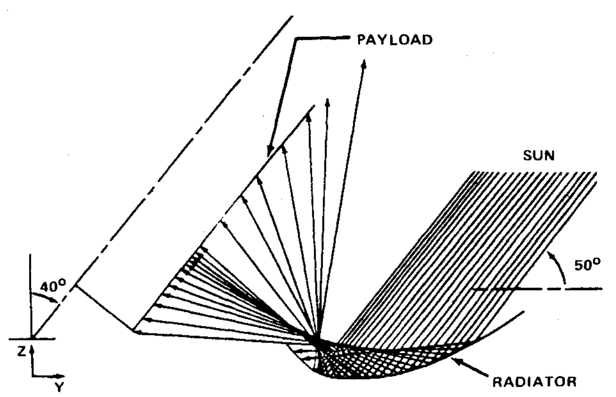

Fig. 5 Most severe cavity created by radiator and SL-2 payload.

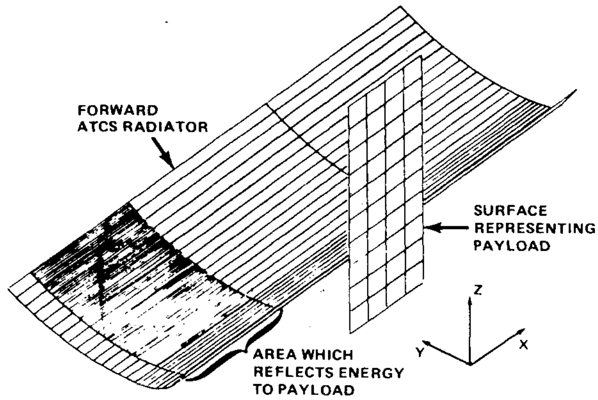

Fig. 7 Three-dimensional TRASYS II based model.

vector is maintained in the yz plane of the Orbiter. However, the hemispherically reflecting nature of a diffuse surface requires the three-dimensional model. This allowed comparison of the diffusely and specularly reflected energy components.

Specular Ray Trace Program

The specialized ray trace program was based on a two-dimensional representation of the radiator and payload geometry. The geometry was identical to the two-dimensional TRASYS II based model. Thus, this program was also limited to a 100% specular radiator. In the program, each straight line segment representing the radiator's contour was characterized by its angle with respect to the xy plane and its location from the payload bay centerline. A single straight line was used to represent the payload. This line was located by its point of origin (with respect to the IPS elevation gimbal) and inclination angle. The geometry relating to this program is shown in Fig. 9. Equations derived from the geometry shown in the figure served as the basis of the program. Heat fluxes absorbed by the payload are calculated by comparing the spacing between incoming rays reflected from the radiators and the same rays when incident on the payload. This computational procedure is depicted in Fig. 10.

Monte Carlo-Based Model

The same geometry as used in the TRASYS II based two-dimensional model was used to predict solar energy distribution on the payload by the Monte Carlo method of random ray generation. Like the two-dimensional TRASYS II based model and the ray trace program, the Monte Carlo model employed in this study was restricted to a 100% specular radiator (although, in general, this restriction does not apply to the Monte Carlo method). Unlike either of the other two methods of analyses (i.e., TRASYS II and the specialized ray trace program), the Monte Carlo method accounts for multiple bounces of a reflected ray.

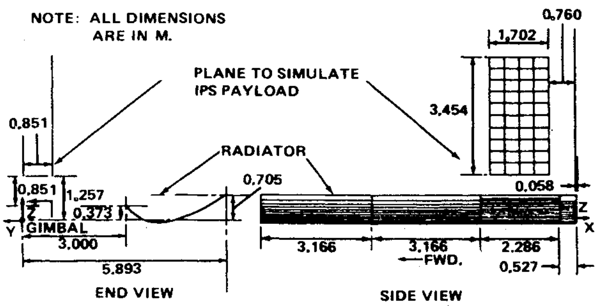

Fig. 8 Three-dimensional TRASYS II based model geometry.

Discussion of Results

Ray Tracings

Using the specialized ray trace program, tracings of rays of solar energy reflected from the radiator surface (parallel to the Orbiter's yz plane) were generated for payload inclination angles ranging from -20 to $+40$ deg (payload inclination angle ψ equals 90 deg minus solar inclination angle β). Two such tracings are presented in Fig. 11. This figure clearly illustrates that, as a result of the radiator curvature, there are areas above the deployed forward radiators where the reflected solar energy is highly concentrated. Figure 12 identifies these areas for the various solar inclination angles considered.

Baseline Case

Using the two-dimensional TRASYS II based model, the data shown in Fig. 13 were generated assuming 100% specular radiators. The heat rates shown in this plot represented solar energy levels reflected from the radiator which were directly irradiated by the sun at an inclination angle of 90 deg. As was characteristic of TRASYS II generated heating rates which were specularly reflected from a nonplanar surface, the data are very discontinuous. Such erratic data result from the representation of nonplanar surfaces (i.e., the radiators) with a series of planar segments. Figure 14 illustrates how planar segments at slight angles with respect to one another can produce overlapping of the reflected image of the energy source. It is these areas of overlapping energy in combination with the nodalization scheme selected for the absorbing surface (the payload, in this study) which produce the spikes of energy (reference, Fig. 13). If it were possible (as well as practical) to utilize an infinite number of planar segments to model the curvature of the radiator, no discontinuities would exist. Figure 15 shows that similar heat rate discontinuities exist when using the Monte Carlo method.

Although discontinuities occurred in the data generated using the two-dimensional TRASYS II based model, it is verified easily by hand calculations that the total energy reflected on the payload as calculated using TRASYS II is accurate. The local heat-flux distribution on the payload was calculated by summing the individual local (i.e., nodal) heat rates shown in Fig. 13 and taking the derivative of this summation. The resulting heat-flux distribution is shown in Fig. 16.

The ray trace program was used to verify the data generated using the two-dimensional TRASYS II model. Figure 16 also compares the payload flux distribution determined with the ray trace program to data generated with the TRASYS II

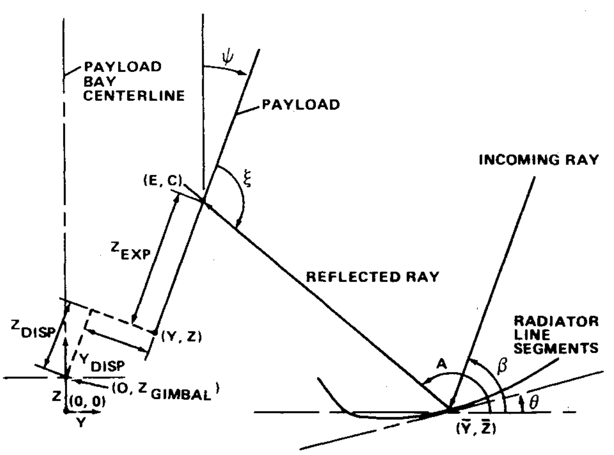

Fig. 9 Specular ray trace program geometry.

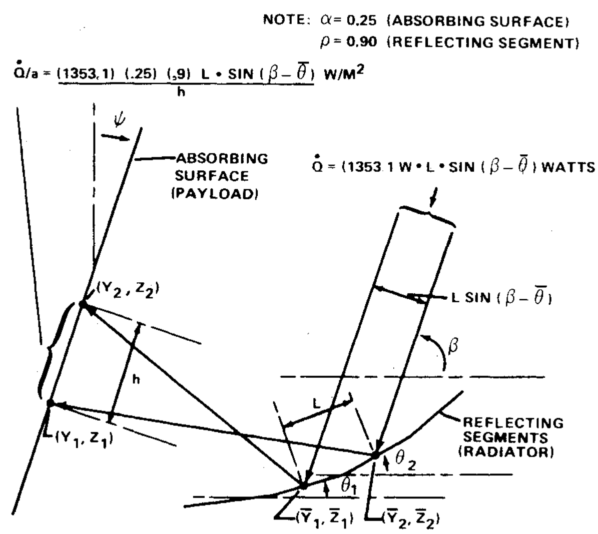

Fig. 10 Heat flux calculation in the specular ray trace program.

model at a 0-deg payload inclination angle. As shown in the figure, these data compare very well.

Payload Inclination Angle Effects

The effect of the inclination angle of the payload was studied using both the TRASYS II two-dimensional model and the ray trace program. The data generated by the ray trace method is shown in Fig. 17. Although data generated with the TRASYS II model are not shown, the data generated by the two methods are very comparable.

Table 1 summarizes the data obtained for the various payload inclination angles studied. The maximum local solar flux on the payload was found to be 76.0 Btu/h-ft^2 (239.7 W/m^2). It was located 4.6 ft (1.4 m) from the base of the payload and found to occur at a 40-deg payload inclination angle. The payload absorbed the greatest amount of solar energy [2800 Btu/h (820.4 W)] at an approximate 14-deg payload inclination angle. The total energy reflected on a single side of the payload decreases as the payload tilts in the direction of a negative payload inclination angle (i.e., the payload tilts away from the radiator). However, although one side of the payload would have no energy reflected onto it at a payload inclination angle of −20 deg, the opposite side (having an inclination angle of +20 deg) would receive 2620 Btu/h (767.7 W).

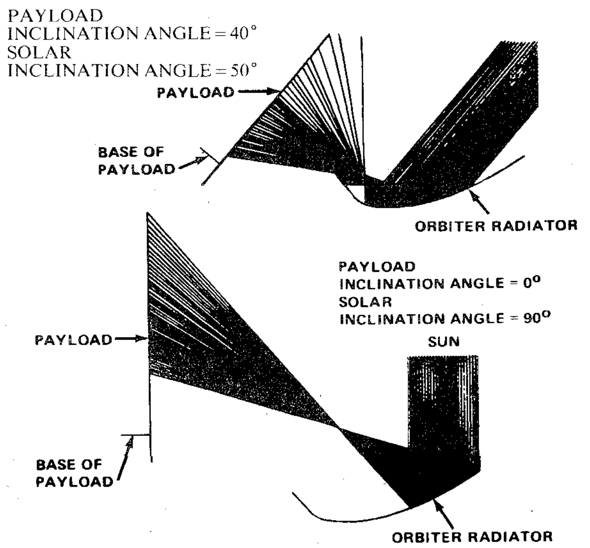

Fig. 11 Tracings of reflected solar energy rays using ray trace program.

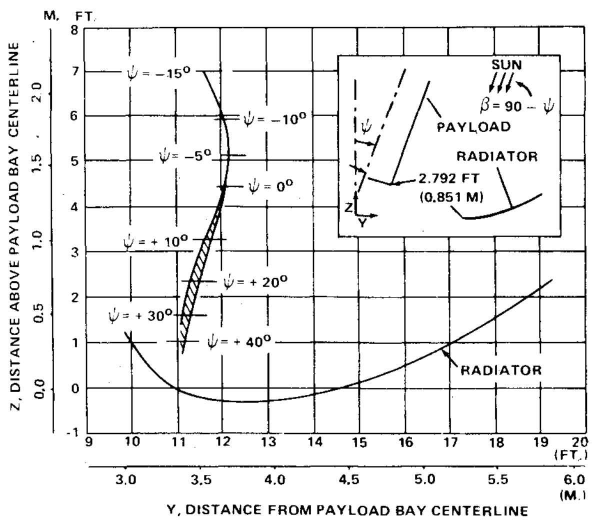

Fig. 12 Areas of highest energy concentration above the deployed forward radiators.

Lateral Payload Location Effects

To determine the amount of solar heat-flux reduction that could be expected on payloads which are located nearer the centerline of the payload bay, additional cases were analyzed to compare with the baseline case [i.e., payload surface located 2.792 ft (0.851 m) off the payload bay centerline in the direction of the radiators]. The analysis showed that a surface at the center of the payload bay has a maximum flux of approximately 80% of that same surface placed 2.792 ft (0.851 m) closer to the radiator. However, the difference in the flux levels approaches zero as one moves up the surface away from the base. The average difference between the two cases is only approximately 10%.

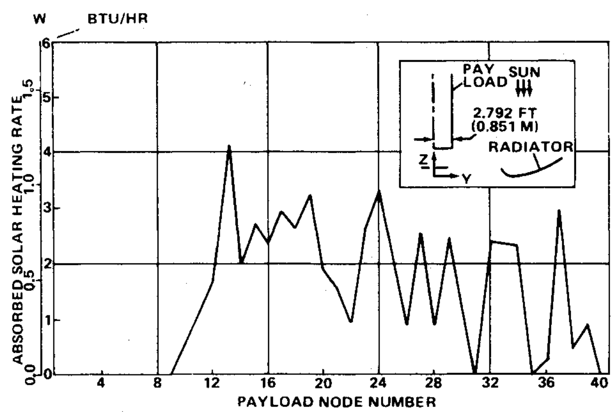

Fig. 13 Payload solar heating rates computed with the two-dimensional TRASYS II based model.

Table 1 Characteristics of solar energy reflected from forward Orbiter radiator for various payload inclination angles

Inclination angle, deg		IPS payload					
		Maximum flux		Maximum flux location[a]		Total energy[b]	
Payload	Solar	Btu/h ft^2	(W/m^2)	ft	(m)	Btu/h	(W)
−20	110	0.0		—		0	
−15	105	38.3	(120.8)	10.45	(3.19)	139	(40.7)
−10	100	53.0	(167.2)	7.20	(2.19)	879	(257.6)
−5	95	64.2	(202.5)	4.92	(1.50)	1425	(417.5)
0	90	70.7	(223.0)	3.23	(0.98)	1917	(561.7)
10	80	63.8	(201.2)	0.70	(0.21)	2639	(773.2)
20	70	52.9	(166.8)	3.35	(1.02)	2620	(767.7)
30	60	62.0	(195.5)	6.07	(1.85)	2166	(634.7)
40	50	76.0	(239.7)	4.60	(1.40)	1680	(492.3)

[a] As measured from the base of the payload.
[b] Assuming 3.454 × 1.702M. ft plane to represent payload.

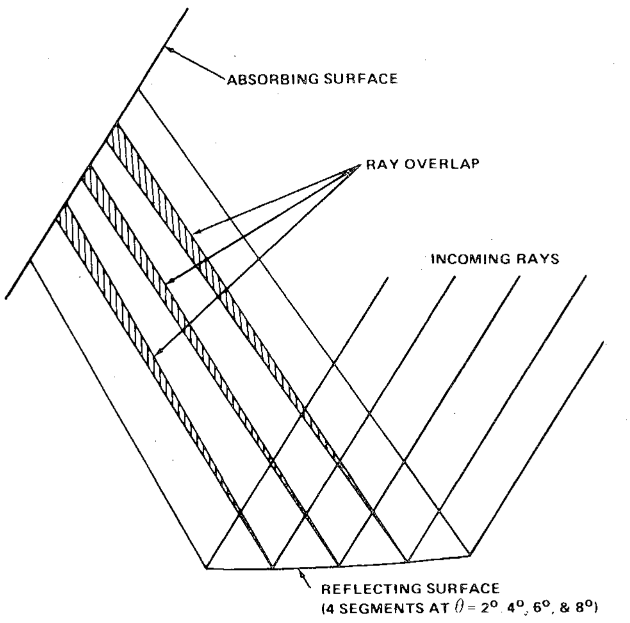

Fig. 14 Reflected ray overlap.

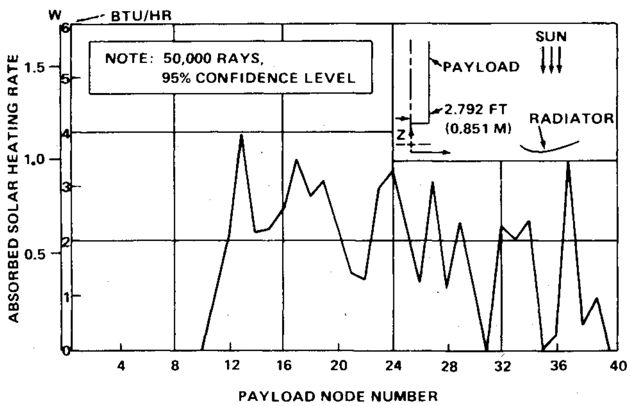

Fig. 15 Payload solar heating rates computed with a Monte Carlo thermal radiation program.

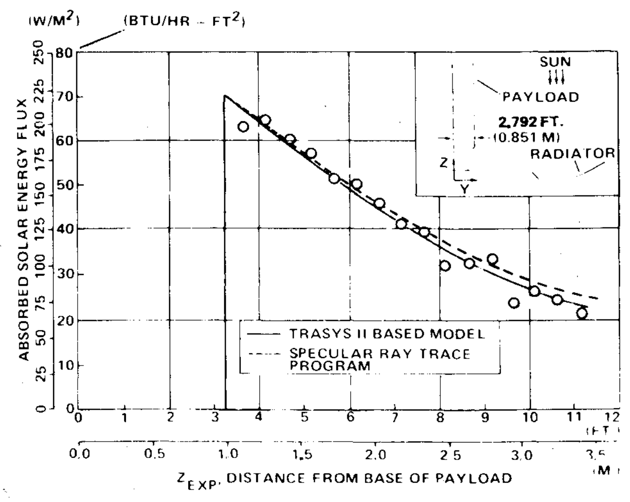

Fig. 16 Payload solar heat flux distribution comparison.

Radiator Specularity Effects

To allow for the uncertainties in the actual specularity of the silverized Teflon when applied to the radiators, the effect of the degree of radiator specularity (i.e., $\%\rho^{\text{spec}}$) on the

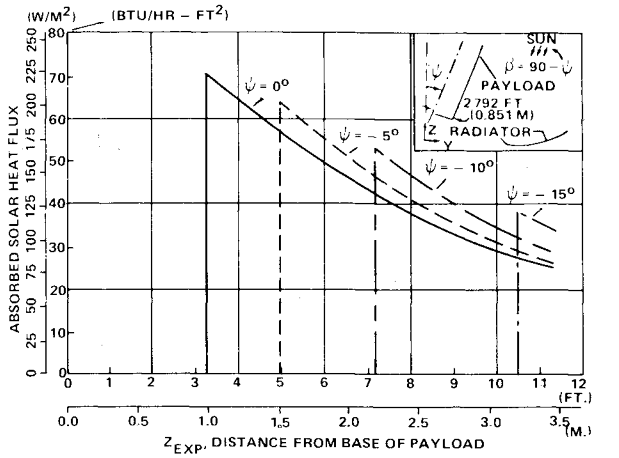

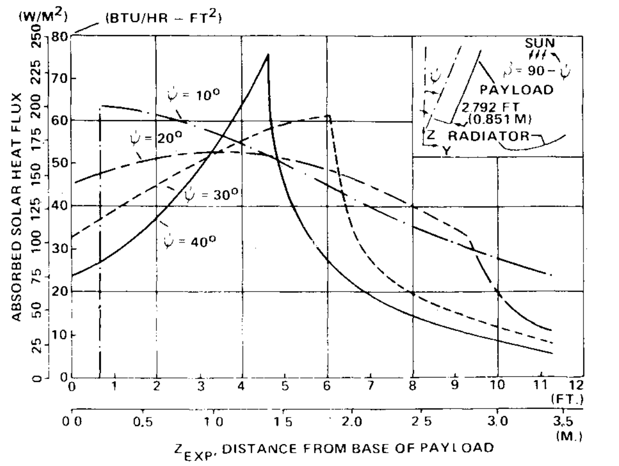

Fig. 17 Payload solar heat flux distribution of various payload inclination angles.

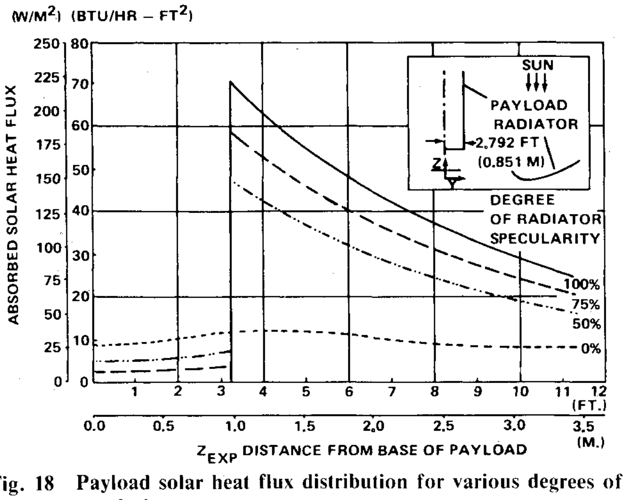

Fig. 18 Payload solar heat flux distribution for various degrees of radiator specularity.

magnitudes of the solar heat flux reflected onto the payload was examined. The three-dimensional TRASYS II based model was used for this task since it is not possible to generate accurate diffusely reflected energy data with a two-dimensional model. Once again, the baseline configuration for this study was taken to have a solar inclination angle of 90 deg. Also, the surface representing the payload was placed 2.792 ft (0.851 m) from the payload bay centerline in the direction of the radiator. Four cases were considered: 0, 50, 75, and 100% specularity of the radiator. The resulting absorbed solar flux data are shown in Fig. 18. Note from the

Table 2 Total payload flux at orbital noon, Btu-h/ft^2 (W/m^2)

	Diffuse radiators	Specular radiators
Maximum	34 (107.2)	93 (293.3)
Average	32 (100.9)	52 (164.0)

figure that the maximum solar flux, considering a 100% specular radiator, is over six times greater than the maximum flux value with a completely diffuse radiator ($\% \rho^{spec} = 0$). As may be seen from the data presented in the figure, because of the increase in the diffuse component of the reflected energy as the radiator specularity decreases, the heat-flux level does not decrease directly in accordance with the reduction in the specularity.

Conclusion

The main conclusion reached from this study is that specular Orbiter radiator reflection must be considered in determining design environments for payloads which can view the forward deployed radiators. Significant error in payload environment definition can occur for elevated payloads in the forward half of the payload bay if the radiators are considered to behave as diffuse reflectors. High local energy levels resulting from reflections from the radiators suggest that in planning future Shuttle mission payload configurations, an attempt should be made to avoid the placement of thermally sensitive payloads which would extend considerable distances above the Orbiter's sill level in the forward half of the payload bay.

The detailed results of this study indicate that payload absorbed heat rates are, in general, significantly higher than would be obtained with an assumption of a diffusely reflecting radiator surface. As an example, using data generated in this study as well as other earlier data, the data in Table 2 are given for a 0-deg payload inclination angle at orbital noon. These data apply to a deployed, white payload orbiting the Earth in a $+z$ solar inertial attitude. The data indicate that when considering specular radiators, the maximum total flux and average flux on an 11.333-ft (3.454-m) high payload located as it was in this study can increase 173 and 63%, respectively, when compared to diffuse radiators. Total flux, as presented in these data, includes all three components of energy normally associated with orbital heating analyses—solar, albedo, and Earth irradiation. In addition, the total flux considers energy reflections of all three energy components. The tabulated values apply at only one point in the orbit (orbital noon). On an orbital average basis, the heat flux is only 47% higher when specular radiators are considered.

Although various analytical methods are available which allow for the consideration of specularly reflecting surfaces, the methods are considerably more complex than those generally used when considering diffuse surfaces. Using current technology, this complexity generally results in much greater computer usage. Also, the methods used in the present study indicated that accurate local heating rates are difficult to predict on surfaces which are heated from energy reflected from specular, nonplanar surfaces. Only by using somewhat cumbersome "smoothing" methods were accurate localized energy levels predictable. There is a definite need for better computer methods for use when analyzing large, complex specular geometries composed of nonplanar surfaces.

References

[1] "Shuttle Vehicle/Spacelab ECS/Thermal Interfaces," NASA Johnson Space Center, Houston, Tex., Doc. ICD-2-05201 (Rev. B), Dec. 1975.

[2] "Lockheed Orbital Heat Rate Package (LOHARP) User's Manual," Lockheed Missiles and Space Co., Huntsville, Ala., LMSC/HREC D162218, April 1970.

[3] "Thermal Radiation Analysis System (TRASYS I) User's Manual," Martin-Marietta Corp., Denver, Colo., MCR-73-105, May 1973.

[4] "Thermal Radiation Analysis System (TRASYS II) User's Manual," Martin-Marietta Corp., Denver, Colo., MCR-73-105 (Rev. 2), June 1979.